VOL.40 Nº2 2023
https://doi.org/10.22491/rmct.v40i2.10970.en

A study of densification and morphology in functionally graded materials of alumina ceramics doped with niobium oxide and silicon dioxide.

Anderson Alves Mota[1], anderson.alves@ime.eb.br
Alaelson Vieira Gomes[1], alaelson@ime.eb.br
[1] Instituto Militar de Engenharia, Rio de Janeiro, RJ

ABSTRACT: *Advanced Ceramic have several applications, among them we could highlight ballistic protection. This usage is mostly due to its mechanical strength and low weight. Alumina (Al2O3), given its characteristics such as easy to obtain and low production cost, represents one of the most researched and used for this purpose of use. However, every material has its own limitation of use, such as low density and bad strength when used without doping. Therefore, solutions have been researched to increase alumina density and improve microstructural to promote better ballistic performance. Even if the homogeneous material get better results, still there is some room for improvement on trying something new. One type of material which has been showing good development is Functionally Graded Materials that could promote a change in characteristics in the same material or that causes a material to behave similar to a ballistic system of several distinct layers, but with the advantage of having no stress concentrators as composites. Thus, this work aims to study the densification of Functionally Graded materials in conventional sintering and to observe microstructure characteristic of the layers in a Scanning Electron Microscope (SEM).*

KEYWORDS: Advanced Ceramics; Alumina; Niobium Oxide; Silicon Dioxide; Functionally Graded Materials.

RESUMO: *As cerâmicas avançadas apresentam diversas aplicações, com destaque para a proteção balística. Elas são bastante utilizadas nesse campo em virtude de apresentarem elevada força mecânica e baixo peso. A alumina (Al2O3), devido a algumas características, como facilidade de obtenção e baixo custo, representa um dos materiais mais pesquisados e utilizados para essa finalidade de emprego. Entretanto, todo material tem limitações de utilização e nem sempre atende a todos os requisitos impostos pela necessidade de utilização. Diante disso, soluções têm sido pesquisadas no sentido de aumentar a densificação da alumina e melhorar características microestruturais para promover um melhor desempenho balístico. Ainda assim, temos oportunidades de melhoria na pesquisa de materiais como no caso de gradiente funcional, promovendo uma mudança de características gradual no mesmo corpo cerâmico, o que faz com que um mesmo material tenha um comportamento semelhante a um sistema balístico de várias camadas distintas de materiais, com a vantagem de não ter as concentrações de tensão desses materiais compósitos. Dessa forma, este trabalho objetiva estudar a densificação de materiais processados a partir da técnica de gradiente funcional e sinterização convencional e observar a característica da microestrutura das camadas e desse gradiente em Microscópio Eletrônico de Varredura (MEV).*

PALAVRAS-CHAVE: Cerâmicas Avançadas; Alumina; Nióbia; Sílica; Gradiente Funcional.

1. Introduction

Ceramic materials have been widely studied and used as ballistic protection mainly due to their characteristics (such as low density and cost and high hardness and durability) that offer them good resistance for a relatively lower density than that of other materials used for this purpose. [1-3]

The development of projectiles with different shapes and great energy has challenged the development of new ballistic materials. This has led to an evolution in advanced ballistic personal protection systems due to their greater demands for new damage-resistant systems that have relative flexibility, weight fit for their use, and an efficient energy absorption capacity. [4]

The evaluation of a ceramic for a given use involves several factors, such as its ability to dissipate energy, physical properties, type of production process, and microstructure. [5]

In general, although silicon and boron carbides have lower densities than alumina (Al_2O_3), this component has more often integrated ballistic vehicle

protection materials due to its simpler processing, lower cost, and better cost/benefit ratio. [6]

Dimensioning a material will ideally enable it to support tensile, compressive, or rotational stresses. Thus, any material in isolation rarely guarantees an adequate response to all types of stimuli, especially during ballistic impacts. [7]

Doping configures an efficient method to minimize these limitations. These components help to control the grain size of alumina during sintering and physical properties such as densification and mechanical strength. [8]

This research developed its alumina-based ceramic system (Al_2O_3) with 4% by weight of niobium pentoxide (Nb_2O_5) at the Military Institute of Engineering ceramic materials laboratory. One of the biggest gains in using this doping material in alumina-based bodies stems from its possibility of reducing the sintering temperature of non-additive alumina from 1600 to 1450°C. This reduction occurs by preserving the mechanical properties of alumina and enabling this system to integrate a ceramic component of ballistic armor. [9-10]

Another method to minimize the limitations of ceramic materials in isolation refers to assembling a multilayer shielding system formed by a first layer of ceramic material and another of a more ductile material, such as fiber-reinforced composites. [11-12]

Such shielding system assembly should improve the behavior of the ceramic material. Japanese researchers proposed another method for the same improvement in the 1980s. They needed to develop a material that would form a thermal barrier as the outer part of the material would be subjected to a temperature of about 2000 K and its inner part would have to remain at 1000 K. Such class of material is now known as functionally gradient materials. [13]

Functionally gradient materials consist of multi-layer materials whose constituents show varying volumetric fractions that are intentionally planned to ensure a progressive change in the microstructure of the material along its length. [14]

An advantage of functionally gradient materials over composites is that the joints of composite materials tend to concentrate stress, at which point most cracks generate delamination. [15]

However, producing a material with a functional gradient by cold uniaxial pressing and conventional sintering can result in materials with laminations and other defects that prevent it from further sintering. [16]

The stress concentrations due to the varying thermal behaviors of the materials in the layers cause such delamination. [17]

The alumina system (Al_2O_3) with 4% of added niobium pentoxide per weight (Nb_2O_5) and the alumina blend (Al_2O_3) with 4% by weight of niobium pentoxide (Nb_2O_5) and 0.8% by weight of silica (SiO_2) show very similar densification properties but considerable hardness differences. [10]

Thus, the main premise of this study is that these mixtures of materials can compose a functionally gradient material for ballistic applications (in which the hardest layer would constitute the impact surface) with great chances of good sintering without cracks and laminations.

Thus, this study aimed to analyze the sintering of ceramic bodies with a functional gradient based on alumina with 4% of its weight of niobium pentoxide (Nb_2O_5), and varying amounts of silica in its compositions (0.04-0.8%) and their densification, emergence of cracks, delamination, and morphology.

2. Materials and Methodology

2.1. Starting Materials

The materials used to produce the samples were: Nb_2O_5, obtained from Companhia Brasileira de Metalurgia e Mineração (Brazil); SiO_2, from the Sibelco brand; and Al_2Or_3 APC 11 SG from the manufacturer Alcoa (Brazil). Moreover, the organic additive Polyethylene glycol (PEG 300) from the company Isofar (Brazil) was added to give consistency to the product.

Table 1 shows the densities of the elements used to make the ceramics:

Table 1 - Density of the constituent elements in the produced ceramics.

Material	Density (g/cm³)
Nb_2O_5	4.60
SiO_2	2.65
Al_2O_3	3.96
PEG	1.13

The density of the powder mixtures was calculated considering the rule of mixtures given by equation 1, which considered the densities of each material and their mass fractions.

$$\rho = \rho_{Al_2O_3} \cdot m_{Al_2O_3} + \rho_{SiO_2} \cdot m_{SiO_2} + \rho_{Nb_2O_5} \cdot m_{Nb_2O_5} + \rho_{PEG} \cdot m_{PEG} \quad (1)$$

In this experiment, three types of powder mixtures were produced with varying percentages of silica mass (Table 2).

Table 2 - Mass composition of the samples.

	Al_2O_3	SiO_2	Nb_2O_5	PEG
Mixture 1	91.6%	0%	3.82%	5%
Mixture 2	90.69%	0.39%	3.8%	5%
Mixture 3	90.84%	0.77%	3.82%	5%

Then, the density of each powder mixture was calculated using Equation 1. The results are shown in Table 3.

Table 3 - Theoretical density of the powders obtained by the rule of mixtures.

Material	Density (g/cm3)
Mixture 1	3.538
Mixture 2	3.529
Mixture 3	3.526

2.2. Sample processing

The materials were added to an alumina-lined jar to homogenize each powder mixture. Deionized water in a mass ratio of 1:1 and alumina balls were added to this material.

This system was taken to a ball mill for eight hours and dried in an oven at 80° C for 48 hours.

After drying, these mixtures were deagglomerated using a pistil and porcelain grail. Then, a sieve shaker was used to obtain the desired grain dimensions. The sieve shaker was run for three-minute periods using a sieve with a 0.355-mm (42 mesh) aperture.

After the three powder mixtures were prepared, these combinations were organized so that they generated seven groups of samples (each with three samples) when pressed. In total, three of these groups were composed of homogeneous materials, one of each mixture of the powders, called "control groups." The other four groups, called "treatment groups," were composed of materials with a functional gradient, three with two layers (groups AB, AC, and BC) and one with three layers (group ABC), according to Figure 1.

Figure 1 - Distribution of samples in the working groups

Favor verificar em qual posição deve ser inserido o texto: niobium pentoxide

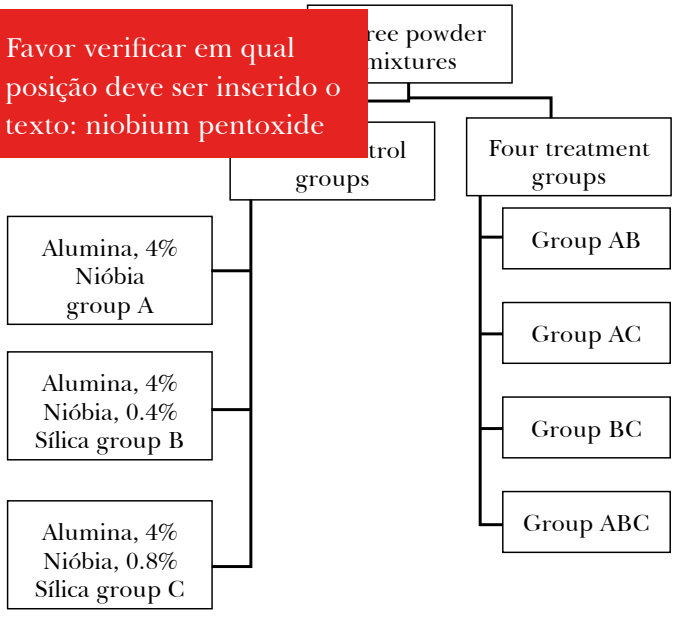

The ceramic bodies were obtained by uniaxial cold pressing in a Skay press with a 30-ton capacity. The ceramic discs were prepared with 47-mm diameter dies using a 50-Mpa load. After pressing, the mass and thickness of each sample were measured.

Homogeneous group samples were pressed in two stages: first a preload was made to settle the material. Then, a main load of about 50 MPa was used to obtain the insert format for the mixture. In the groups whose samples consist of materials with a functional gradient, a preload was performed for each layer of the material; then, a main load of 50 MPa was made.

Sintering was carried out in two stages. In the first one, the binders were evaporated following Figure 2.

Figure 2 - Binder evaporation route

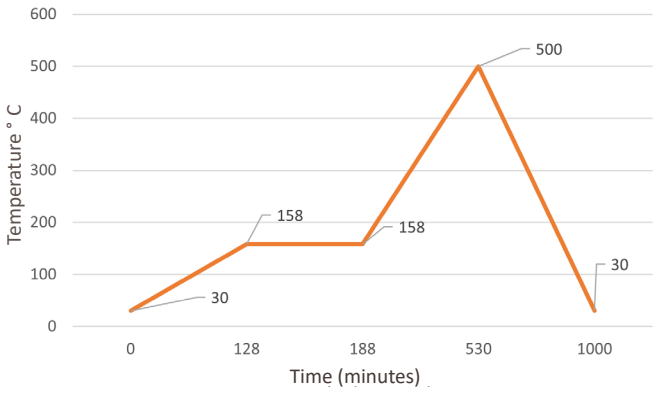

Then, the materials were placed in a Flyever INTI furnace with a FE50RPN controller to sinter the samples, according to Figure 3.

Figure 3 - Sintering route

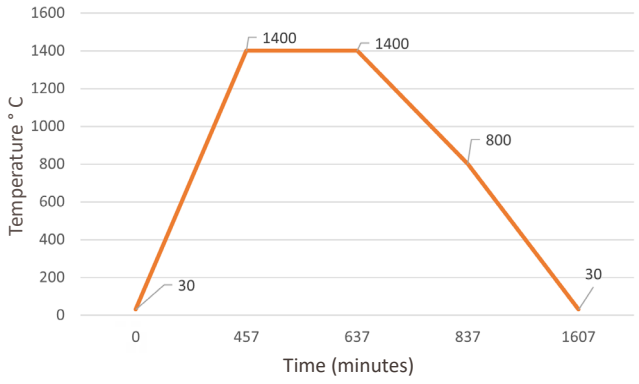

Then, after the sintered ceramic bodies were obtained, the characterization stages were carried out.

2.3. Characterization

2.3.1. Green density

From the theoretical densities in Table 3 and the masses and thicknesses measured after pressing, the green density and densification were calculated by Equation 2 and 3.

$$\rho_{green} = \frac{m_{sample}}{V_{sample}} \quad (2)$$

$$Desinfication_{green} = \frac{\rho_{green}}{\rho_{theoretical}} \cdot 100\% \quad (3)$$

2.3.2. Densification of Sintered Samples

Apparent and relative densities were calculated by the Archimedes method according to NBR 16667:2017 [18], using the measurements of immersed mass (m_i), wet mass (m_w), and dry matter (m_d), in which m_l represents the specific mass of the distilled water: 1 g/cm³. With these parameters, the bulk and relative densities were evaluated by Equations 4 and 5 and the theoretical density of the body obtained by Table 3.

$$d_a(g/cm^3) = \frac{m_s}{m_u - m_i} \cdot m_l \quad (4)$$

$$\rho_{relative} = \frac{d_a}{d_{theoretical}} \quad (5)$$

2.3.3. X-ray Diffraction (XRD)

X-ray diffraction analysis was performed at IME using a Panalytical Xpert MRD diffractometer under Co-Kα radiation and a power of 40 kVe.

The starting powders and the sintered samples were thus analyzed: In the samples of groups 1, 2, and 3, this analysis was performed on only one side

of the sample. In the samples of groups 4, 5, 6, and 7 (those with functional gradients), it was performed on both sides. A 30-mA current and a 5-to-80º scan were used as test parameters.

2.3.3. Scanning Electron Microscopy (SEM)

After the samples were fractured, the fracture surface was analyzed by SEM to obtain more information about the microstructure of the material and the interface of the layers of the functional gradient groups.

This analysis was performed in a QUANTA FEG 250 scanning electron microscope, in which a beam of 20 kVe and 5 µm in diameter was used. The increases were standardized at 1000, 5000, and 10,000 ×, except for cases in which the fractured surface was attempted to be observed as a whole, in which case 35 and 75 × were used.

3. Results and discussion

3.1 Green densification of Samples

Table 3 describes the green densification of the analyzed sample sets.

Table 4 - Green density of the samples.

Groups	Density (g/cm³)	Green densification (%)
Group A	2.449 ± 0.043	68.57 ± 1.26
Group B	2.385 ± 0.018	67.32 ± 0.54
Group C	2.328 ± 0.055	65.73 ± 1.34
Group AB	2.384 ± 0.029	67.05 ± 0.81
Group AC	2.382 ± 0.033	66.85 ± 0.93
Group BC	2.374 ± 0.017	66.87 ± 0.40
Group ABC	2.374 ± 0.032	69.10 ± 0.90

The results show that adding silica decreased the densification of the ceramics by up to 2.84%, as in the literature [10]. The densification of the groups with functional gradient showed varying behavior in all cases. The ABC group stands out for having the highest densification, an expected result since each layer increasingly resist packaging and arrangement. Another important point is that all green densities averaged higher than 55%, the minimum level for good sintering.

3.2 Densification of sintered samples

Table 5 describes the results of relative density of the samples after sintering.

Table 5 - Relative densification of the sintered samples.

Groups	Relative humidity (%)
Group A	90.28 ± 0.75
Group B	88.26 ± 3.77
Group C	87.85 ± 5.42
Group AB	92.25 ± 3.75
Group AC	91.17 ± 3.30
Group BC	90.98 ± 1.55
Group ABC	93.23 ± 0.45

The results in Table 5 show a decrease in the densification of the material as silica was added, as in the literature [10,11].

Functional gradient samples averaged better densities than those with homogeneous material. The samples in the ABC group (three layers of material) again stand out for their densification. The greater number of layers increased sample densification, unlike the literature [16].

3.3 X-ray Diffraction (XRD)

Figures 4, 5, and 6 contain the diffractograms of each powder before pressing and sintering. Their mixtures show peaks corresponding to alumina, niobium pentoxide, and silica. This suggests no impurities in the starting materials, which could impair densification or cause reactions that would change the microstructure of the sintered material and the mechanical behavior of the final ceramic body.

Figure 4 - XRD of powder mixture A

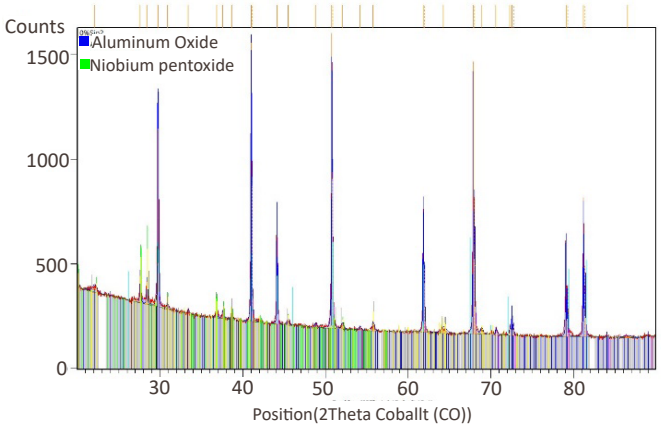

Figure 5 - XRD of powder mixture B Figure 4 – XRD of powder mixture A

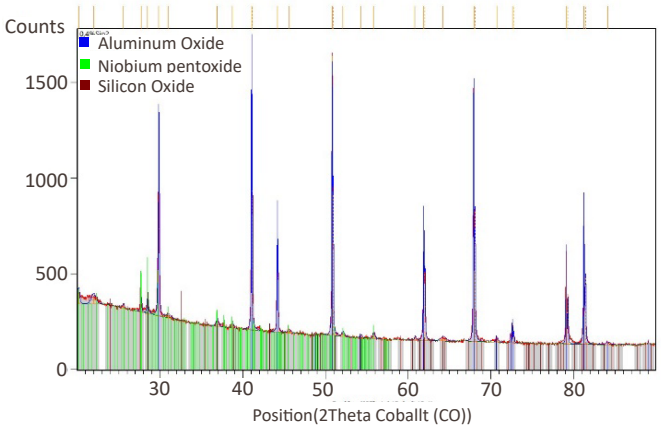

Figure 6 - XRD of powder mixture C Figure 4 – XRD of powder mixture A

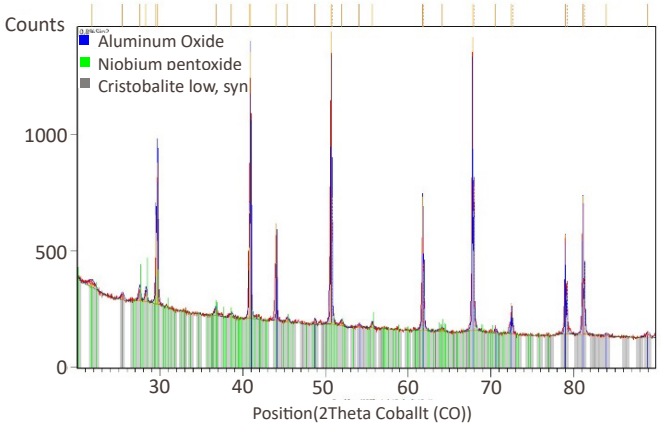

The diffractogram of the sintered samples indicated the presence of some phases in addition to those phases in the XRD of the powders.

A phase that plays a fundamental role in the greater densification of alumina by adding niobium pentoxide refers to aluminum niobate. This phase occurred in basically all sintered sample groups, as per Figure 7.

Figure 7 - XRD synthesized group A sample Figure 4 – XRD of powder mixture A

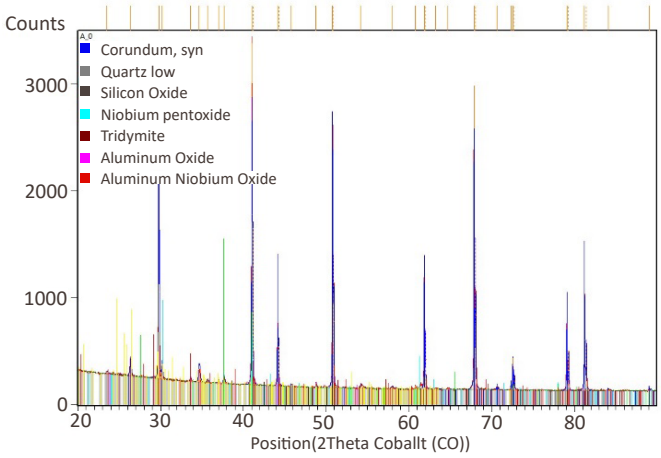

3.4 Scanning Electron Microscopy (SEM)

SEM at 1000-, 5000-, and 10000-× magnification obtained micrographs of the fractures in the materials. In the samples from the groups with functional gradient, analyses used a 35-× increase.

The image with a 35-× magnification shows satisfactory performed material compaction and sintering and no discontinuity in the transition between the material layers.

It also shows a predominantly intergranular fracture, which, in general, is inherent to materials with better impact energy absorption [10].

It also showed a greater porosity on the side of material C, which has 0.8% silica. This agrees with the densification of the material in this study.

Finally, an average grain size occurred on the side of material A, which shows that the silica influenced grain growth by mullite. [10]

Figure 8 - Image of the fracture of the ABC group material on the A-side of the material

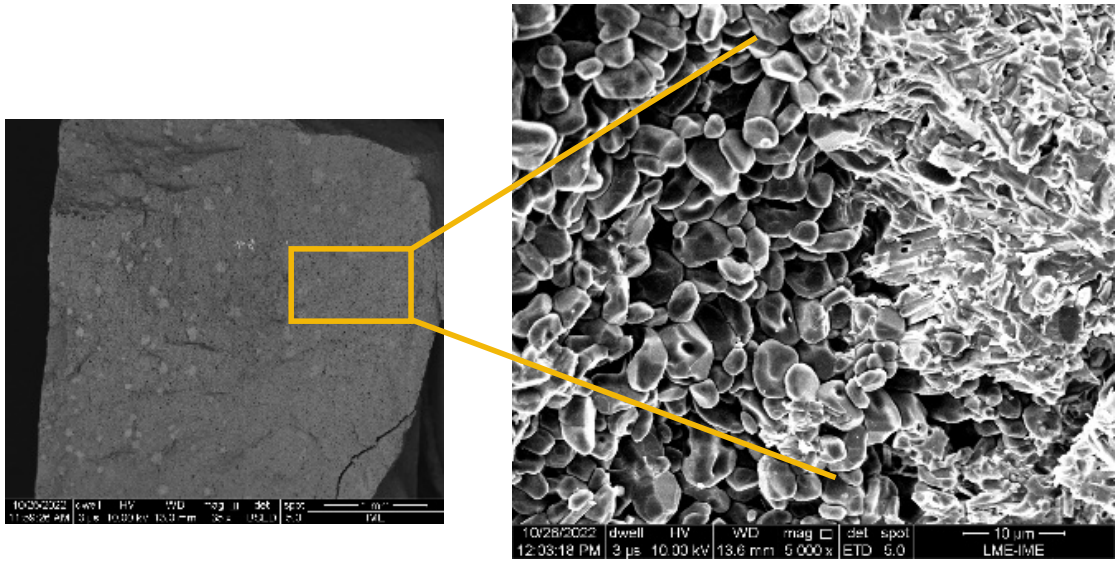

Figure 9 - Image of the fracture of the ABC group material on the C side of the material

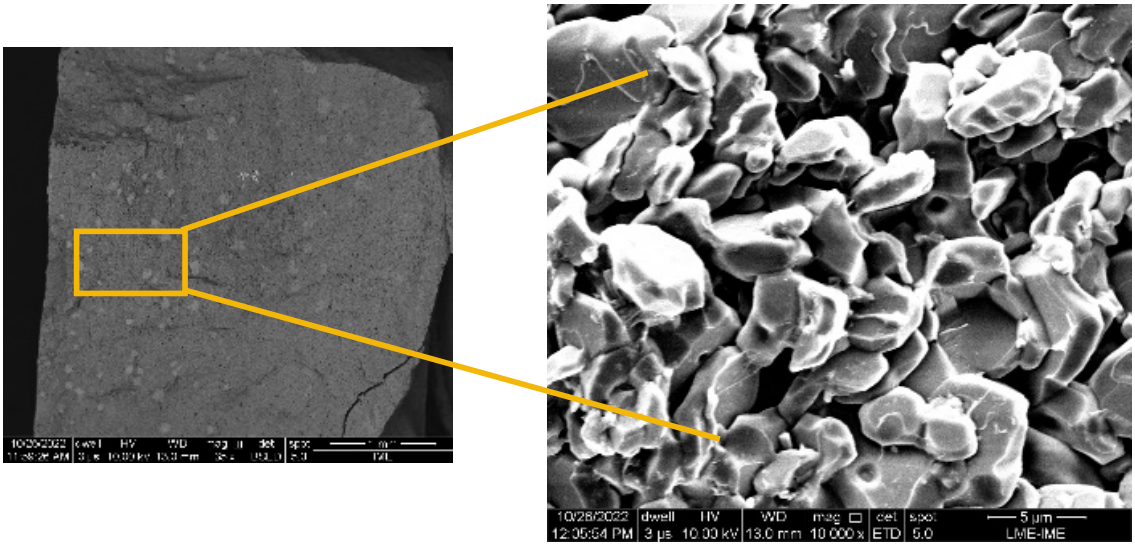

4. Conclusions

This study produced advanced ceramics from three mixtures of alumina powders in which 4% of their mass comprised niobium pentoxide and a variable composition of silica (0, 0.4, and 0.8%). These powder mixtures resulted in seven groups of ceramic bodies, each with three samples. The increase in layers may have influenced the increase in material densification. The materials with a higher presence of silica had a lower densification. Finally, cold uniaxial pressing with sintering in a conventional furnace showed success since the sintered samples showed no delamination and the transition of the material layers had no discontinuity in the SEM.

References

[1] APPLEBY-THOMAS, G. J. et al. Fitzmaurice, On the effects of powder morphology on the post-comminution ballistic strength of ceramics. International Journal of Impact Engineering, Amsterdam, v..100, p. 46-55, 2017.
[2] KOBAYASHI, A. Characteristics of high hardness alumina coatings formed by gas tunnel plasma spraying. Journal of Thermal Spray Technology, Berlin, v. 5, n. 3, p. 298-302, 1996.
[3] BAUDÍN, C.; TRICOTEAUX, A.; JOIRE, A. Improved resistance of alumina to mild wear by aluminium titanate additions. Journal of the European Ceramic Society, Amsterdam, v. 34, p. 69-80, 2014.
[4] YADAV, R. et al. Body armour materials: from steel to contemporary biomimetic systems. RSC Advances, London, n. 116, p. 115145-115174, 2016.
[5] MEDVEDOVSKI, E. Ballistic performance of armour ceramics: influence of design and structure. Part 1. Ceramics International, v. 36, n. 7, p. 2103-2115, 2010.
[6] CARTON, E..et al. Inertia as Main Working Mechanism for Ceramic Based Armour. Journal Contribution, [s. l.], 2019.
[7] SILVA, M. V. et al. Blindagens Cerâmicas para Aplicações Balísticas: uma revisão. Cerâmica, São Paulo, v. 60, n. 355, p. 323-331, 2014
[8] MILAK, P. et al. The influence of dopants in the grain size of alumina – A review. Materials Science Forum, Bäch, v. 820, p. 280-284, 2015.
[9] GOMES, A. V. Comportamento balístico da alumina com adição de nióbia e variação da geometria do alvo. Tese (Doutorado em Ciências dos Materiais) –,Instituto Militar de Engenharia, Rio de Janeiro, 2004.
[10] GOMES, A. V. Comportamento Balístico de alumina com adições de nióbia, sílica e magnésia. Dissertação (Mestrado em Ciências dos Materiais) – Instituto Militar de Engenharia, Rio de Janeiro, 1999.
[11] BÜRGER, D. et al. Ballistic impact simulation of an armour-piercing projectile on hybrid ceramic/fiber reinforced composite armours. International Journal of Impact Engineering, Amsterdam, v. 43, p. 63-77, 2012.
[12] NASCIMENTO, L. F. C. Caracterização do compósito de epóxi/fibra de malva para emprego em blindagem balística multicamada. Tese (Tese de Doutorado) – Instituto Militar de Engenharia, Rio de Janeiro, 2017.
[13] MAHAMOOD, R. M. et al. Functionally graded material: an overview. International Association of Engineers (IAENG), 2012.
[14] Shanmugavel, P et al. An overview of fracture analysis in functionally graded materials. European Journal of Scientific Research, [s. l.], v. 68, n. 3, p. 412-439, 2012.
[15] WANG, S. S. Fracture mechanics for delamination problems in composite materials. Journal of Composite Materials, Thousand Oaks, v. 17, n. 3, p. 210-223, 1983.
[16] JESUS, P. R. R. Processamento e caracterização de um material cerâmico à base de alumina com gradiente funcional para aplicações balísticas. Tese (Doutorado em Ciências dos Materiais) – Instituto Militar de Engenharia, Rio de Janeiro, 2021.
[17] LEUSHAKE, U. et al. General aspects of fgm fabrication by powder stacking. In: TRANS TECH PUBL. Materials science forum. [S.l.], 1999. v. 308.
[18] ABNT – Associação Brasileira de Normas Técnicas. ABNT NBR 16661:2017: Material refratário denso conformado – determinação de volume aparente, volume aparente da parte solida, densidade da massa aparente, densidade aparente da parte solida, porosidade aparente e absorção. Rio de Janeiro: ABNT,.2017.